Zeitschrift: Helvetica Physica Acta
Band: 30 (1957)
Heft: II-III

Artikel: Nuclear levels and shell structure
Autor: Bleuler, K. / Terreaux, Ch.
DOI: https://doi.org/10.5169/seals-112812

Nuclear Levels and Shell Structure

by **K. Bleuler***) and **Ch. Terreaux**

Seminar für theoretische Physik der Universität Zürich.

(3. I. 1957.)

Summary. The experimental results concerning binding energies and level schemes from all heavier odd neutron nuclei ($A > 30$) are studied: A new graphical method is introduced in order to obtain a comprehensive survey of these values throughout the periodic table by means of a system of curves. With the help of this geometrical representation a detailed comparison with the corresponding results from the shell model is made: There is a striking agreement in a large part of the periodic system. Typical deviations are found in the domain of large level density of the spherical shell structure (corresponding to the region of deformed nuclei). From this comparison it is possible to determine a phenomenological expression for the spin orbit coupling term. This interaction agrees with the results obtained from an analysis of the scattering of polarized protons. It is then proved that the same coupling law also holds in the region of light nuclei. Some preliminary considerations about the pseudoscalar meson field in relation to our large spin orbit interaction are given at the end of the paper.

1. Introduction.

1. A Survey. A large amount of nuclear data (level schemes, charge distributions, binding energies etc.) has been accumulated during the past years. So far, no complete theory is available, but several nuclear models have been proposed which in general apply to different regions of the periodic table. They constitute an interesting intermediate stage (a kind of phenomenological view-point) which should lead, eventually, to a more fundamental theory of nuclear structure. It is, therefore, important to decide about the validity of these models by means of a systematic comparison with the experimental results. This analysis should include the determination of the characteristic parameters (e. g. the depth and the radii of the

*) Now at the University of Neuchâtel, Neuchâtel (Switzerland).

potential wells introduced in the case of the shell model), as well as an estimate of the domains in which the different models may be applied.

The main purpose of this work is a detailed comparison between the experimental data from all heavier odd N nuclei (A from 30 to 210) and the corresponding results from the shell model. The first part, therefore, contains a general analysis of the experimental values concerning level schemes and binding energies by means of a new graphical method. This geometrical scheme provides a comprehensive survey of nuclear properties in a large part of the periodic table. The resulting 'two-dimensional' level scheme (the average separation energies corresponding to all nuclear states with the same assignment are plotted as functions of the neutron number N; compare fig. 5) is very suitable for making a systematical comparison with the theoretical values. Next, we consider the shell structure: We use the Hofstadter results concerning the charge distributions and the Weisskopf Feshbach analysis of the neutron scattering, in order to determine the parameters of the potential wells. We then calculate the single particle levels for the whole sequence of potentials occurring in the periodic system. (In this case, the eigenvalues are 'functions' of the neutron number.) The resulting theoretical 'two-dimensional' level scheme is also presented in graphical form. Thus, the comparison can be made immediately (fig. 5): There is a striking similarity between the two systems of curves. Several conclusions will be drawn from this fact.

Now, we can estimate the domains in which the shell model (in a somewhat generalized sense, taking the effect of admixtures into account) constitutes a reasonable approximation. It is also possible to determine an important parameter: The magnitude of the spin orbit coupling term. Furthermore, the region in which the comparison can be made is so large (i.e. the shape of the potential exhibits such a large variation) that we were also able to decide about the type of spin orbit interaction which must be assumed: It is the well-known law (4) containing the gradient of the nuclear potential. This coupling type results from an invariant interaction of the nucleon with any scalar field. In view of the very strange numerical value, we also study other cases. We thus show that the same law leads to a satisfactory agreement with some experimental results from the region of light nuclei, although nuclear structure is rather different in this domain. Here, our interaction is seen to be valid, too, for the protons. In a later paper it will be shown that the same coupling also holds for all heavier, odd proton nuclei. Even-

tually, the spin orbit interaction has been estimated from the nuclear scattering of polarized protons (azimutal angular dependence). The analysis of the experimental results[10]) from various nuclei leads practically to the same magnitude of this coupling, in spite of the fact that the energies involved are much larger in these experiments.

In earlier work, the comparison between the shell model and the experimental level structure of nuclei was chiefly based on the usual one-particle level scheme, which had been introduced in order to represent the characteristic sequence of assignments for states of odd nuclei. We might call it in this connection a 'one-dimensional' scheme. An accurate representation may be found in an article by KLINKENBERG[1]). In a previous paper[2]) (quoted here as paper I) shell structure has been worked out in some detail: Charge distributions, radii, binding energies and the depth of nuclear potentials were studied within the framework of this model. As a result, a much more general scheme of the single particle levels was obtained: The energies of the one-particle levels were determined numerically as a function of the atomic number. From this 'two-dimensional' scheme, several typical experimental features of nuclei were immediately noticed: The energy steps at the positions of the magic numbers, groups of narrow lying levels, and, in some special cases, their overcrossings if one looks through the periodic system. We then realized that this type of level scheme was very useful even from a phenomenological view-point, in order to obtain a survey of nuclear properties. Therefore, the question arose whether it might be possible to construct such a 'two-dimensional' scheme directly from the corresponding experimental results. These considerations were at the origin of our present work.

2. The method. Our graphical method is based on the following argument: In the shell model the parameters of the nuclear potential are smooth functions of N and Z (neutron and proton numbers looked upon as continuous variables; the radius law (3) constitutes a typical example). We then consider the energy eigenvalues E_n of the single particle states corresponding to these potentials: they are also smooth functions ($E_n(N, Z)$) of N and Z and they can, therefore, be represented by a system of surfaces within a 3-dimensional space (the coordinates being E_n, N, Z). To every surface corresponds the characteristic single particle assignment denoted by j^P (total angular momentum $j = l \pm \frac{1}{2}$, parity P determined by the parity of l). Now, according to the principles adopted in shell structure (compact occupation of the single particle states up to the Fermi level) these surfaces represent the variation of the ionization (or

separation) energies for a sequence of nuclei which correspond to the same Fermi level*). If the ground states of these nuclei are single particle states, j^P represents at the same time the total assignment. If, in addition, the zero line for E_n is defined conveniently, our energy axis stands for the separation energy. We then write $\tau_{jP}(N,Z)$ instead of $E_n(N,Z)$, putting the corresponding assignments in evidence. Thus, within this frame, our eigenvalue surfaces directly show some properties of nuclear ground states. Our surfaces, however, also contain excited single particle states of neighbouring nuclei. In this case τ_{jP} represents the ionization energy, plus (for holes) or minus (for ordinary states) the excitation energy of the nuclear state in question*).

So far, we have considered the ideal shell structure; admixtures resulting from the direct interaction between the nucleons (treated as a perturbation of the single particle states) have yet to be taken into account. Our main conjecture states that these admixtures will only cause continuous deformations of our surfaces (no breaks). We shall even see that no major interchanges will occur. Now, it is quite obvious that these 'generalized' surfaces can also be constructed directly with the help of the experimental results concerning binding energies, assignments and excitation energies. (The ionization energies may be determined from the differences of the binding energies of consecutive nuclei.) The detailed rules for this construction will be given in section 2. For practical reasons we represent our energy surfaces by means of a set of intersections $Z = \text{const.}$ projected on the (τ, N)-coordinate plane. In this way a large amount of nuclear data can be incorporated into a system of curves covering an important part of the periodic table. The mere fact that we really find a continuous system of curves shows, in some way, the validity of our model. (For example our construction would not work in the case of Russel Saunders coupling, i.e. for the electronic shell.)

In order to simplify our comparison with the theoretical results, we construct our reduced two-dimensional system of the 'mean value curves': In the (N, Z)-plane we consider a smooth curve representing the middle line $\overline{N}(Z)$ of the flow of stable elements. Only for nuclei situated near this line the parameters of the potential wells are approximately known. Therefore, the comparison will be made for the (ideal) nuclei situated on this line. We thus consider the corresponding energy values τ_{jP}: In this way a mean value curve (determined by the projection $\overline{N}(Z)$ on the (N, Z)-plane) is defined

*) Compare fig. 1. A complete geometrical representation will be given in a special paper.

on each energy surface. Again, we represent these mean lines with the help of the projections on the (τ, N)-plane. We thus obtain in this plane our system of mean value curves, each being characterized by the assignment j^P of the generating nuclear states. This system constitutes our 'two-dimensional' level-scheme which will be compared to the corresponding theoretical diagram (fig. 5).

Our next task (section 3) is to make numerical calculations based on the shell model. They have been carried out along the same lines as in paper I (graphical integration of the radial equations), but it was most important to introduce a new radius law (in accordance with the new Stanford results) and a different definition of the zero line for the potentials. In these calculations we introduce from the very beginning a relation between N and Z (according to the middle line in the (N, Z)-plane) in order to reduce the variety of eigenvalue problems which must be solved. Furthermore, the radius law (3) may not be valid outside our middle line and the potential depth exhibits a strong variation as one moves away from this line. The eigenvalues (a suitable spin orbit term being included) are now functions of one variable only (we choose N), each function being characterized by the corresponding assignment j^P. This constitutes our theoretical (two-dimensional) scheme.

3. The Results. The results from our comparison (details are given in section 3) may be summarized as follows:

(a) An appreciable part (about 80%) of all low-lying nuclear states fit into our scheme; this means that a large number of states may indeed be interpreted (in a generalized sense) as single particle states.

(b) The effect of admixtures is rather large: Especially in the middle regions of the shells, the distances between the experimental levels are different from the calculated ones. Even near the very edges of the closed neutron shells the admixtures due to proton states alone are strongly felt. However, the sequence of states and the relative level spacings are really quite similar in both cases. In particular, the energy steps situated at the positions of the magic numbers are still very conspicuous in the experimental scheme, although they are reduced by a factor of about two if compared to the theoretical values. For these reasons a comparison in a small part only of the periodic table would show little similarity. It is rather our 'large scale' survey which shows that shell structure constitutes a rough 'first order approximation' in a large part of the periodic system.

(c) There are some 'ideal' nuclei situated near the double magic structures (small admixtures!). We therefore expect a numerical agreement for the excitation energies of these nuclei. This is really the case (compare table I).

(d) There is a region of very large density of the theoretical single particle levels. (N from 90 to 115 and the corresponding Z from 60 to 75; compare fig. 5. In this region the proton scheme also exhibits a large level density. This scheme being somewhat different from the neutron system will be reproduced in a future publication.) The perturbing individual interactions between the nucleons may, therefore, completely change the nuclear structure. In fact, this region corresponds precisely to the domain of deformed nuclei[11]).

(e) We use the same invariant law (4) for the spin orbit coupling all over the periodic table (below and above the break caused by the deformation). It is easily seen that our results depend in a rather sensitive manner on the magnitude and the analytic form of this interaction (more details about this point will be given in a later paper). For these reasons we were able to determine the spin orbit interaction rather accurately (compare (4) section 3); in addition it was seen that the best fit was obtained with a unique law for the interaction.

In order to complete this investigation, we extend our analysis to the domain of light nuclei. Although no shell structure can be assumed here, there are some special cases where the effect of the spin orbit coupling may be seen directly. Those are the nuclear 'alcalide structures' in which one extra particle is moving in the central field generated by a stable core (e.g. O^{17} with the core O^{16} etc.). There is, in fact, an enormous doublet splitting observed in these cases; but a rather careful analysis of these level schemes is needed because of the existence of a large exchange interaction of the extra particle with the core, which must be taken into account (see section 3). We then realized that our interaction (4) gave a satisfactory agreement in all cases (compare fig. 9).

We thus find the same law for the spin orbit coupling in very different cases (for protons and neutrons in a region extending from very light to extremely heavy nuclei). According to this law our coupling depends only on the field in which the particle is moving. This field may be generated by completely different nuclear structures. For this reason it seems rather unlikely that the spin orbit splitting could be indirectly produced by the twobody tensor forces: This effect *would* depend on the structure of the whole system. On the other hand, our numerical value of the spin orbit coupling is

much larger than the relativistic term which is obtained from the interaction of nucleons with a scalar field. It seems, however, very likely that the interaction with a pseudoscalar field will give the right order of magnitude. From the standpoint of an approximate nuclear theory (a classical meson field representing the nuclear potential) this fact is in perfect agreement with the well-known properties of the pion.

§ 2. Graphical representation of energy levels.

In this section our graphical method representing ground states and low-lying levels of odd nuclei will be treated. We use the following experimental data: Binding energies B (values according to WAPSTRA[3]) and HUIZENGA[4]), assignments (angular momentum quantum number and parity, abreviated by j^P) and excitation energies (level schemes[14]). We have already seen that the shell model

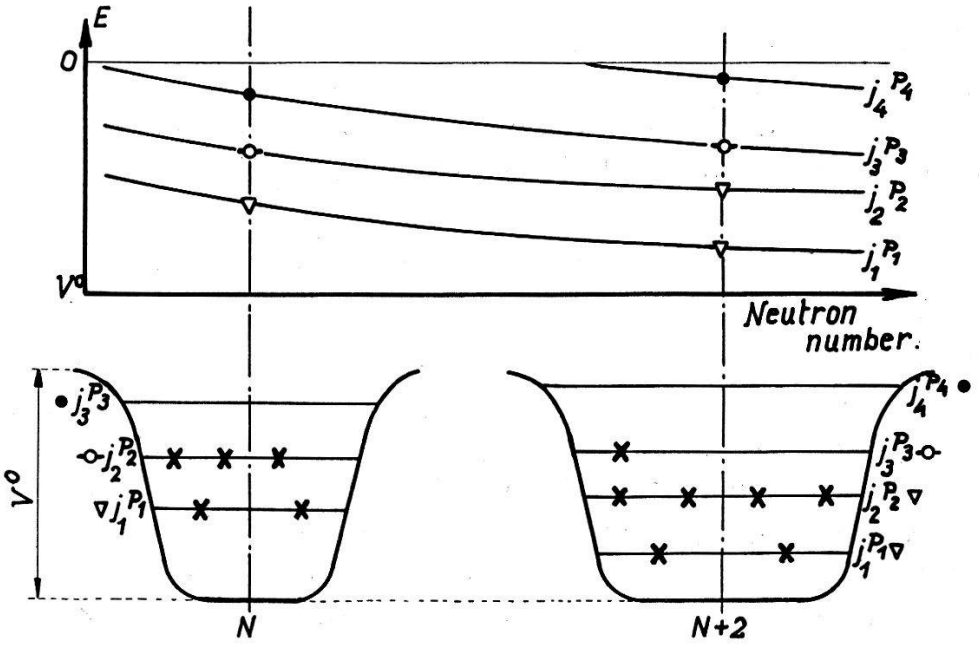

Fig. 1.

A schematic representation of the behaviour of levels according to the shell model.

The levels are shown for two consecutive odd nuclei (N and $N+2$, -o- = ground state, • = ordinary excited state, ▽ = hole state, $j_1^{P_2}$ etc. are different assigments). In the bottom part the potential wells and the corresponding levels are drawn; a compact occupation by nucleons has been indicated. Above, nuclear levels are drawn as functions of N. For example, the point -o- on the $j_2^{P_1}$ curve is the ground state of the smaller nucleus N (one unpaired neutron in the $j_2^{P_2}$ shell), and the point ▽ on the same curve is a hole state of the nucleus $N+2$ where the $j_2^{P_2}$ shell is already filled in the ground state. The actual excitation energy has to be inserted with opposite sign if compared with the ordinary excited states.

*

suggests (with the help of these data) the construction of a system of curves representing the energy levels as functions of the neutron number N (compare fig. 1). In this way a complete survey of nuclear properties will be obtained. It will then be possible to check in some detail the predictions of the shell structure and to determine some fundamental values relevant to it. Our construction is based on the following principles (it is worked out here for the odd neutron case):

A. *Representation of ground states.*

For every isotope (odd N) for which the experimental assignment j^P of the ground state is known, we determine the minimum ionization (separation) energy τ_{jP} with the help of the difference of the binding energies B of consecutive odd nuclei; we put

$$\tau_{jP}(N,Z) = \frac{1}{2}\{B_{jP}(N,Z) - B_{jP}(N-2,Z)\}. \qquad (1)$$

In this way we only compare nuclei with similar properties (odd N, in general with the same assignment j^P). This would not be the case if we had used the usual definition

$$\tau' = B(N,Z) - B(N-1,Z)$$

which is not suitable for our method. These values τ_{jP} are then plotted on the vertical axis of our diagram as 'functions' of the neutron number N. (Fig. 2 is a schematic representation of this plot). It is then seen that all points which correspond to the same values of Z and j^P lie on smooth curves K_{Zj^P}. In this way the whole periodic table is covered with a system of regular curves, each corresponding to a set of isotopes with the same values for Z and j^P. (Fig. 3 shows a small part of this extensive diagram for the interval $N = 35$—65; the complete diagram will be reproduced in a special publication.) It is now readily seen that curves corresponding to the same assignment j^P but to different values of Z (Z, $Z+2$, $Z+4$...) are very similar. They form a regular sequence with nearly equal distances (see fig. 3). For this reason we may define characteristic sub-systems each corresponding to a given assignment j^P. This behaviour corresponds perfectly to the special properties of shell structure: These sub-systems represent in fact our energy surfaces (defined in section 1) by means of a sequence of intersections $Z = \text{const.}$.

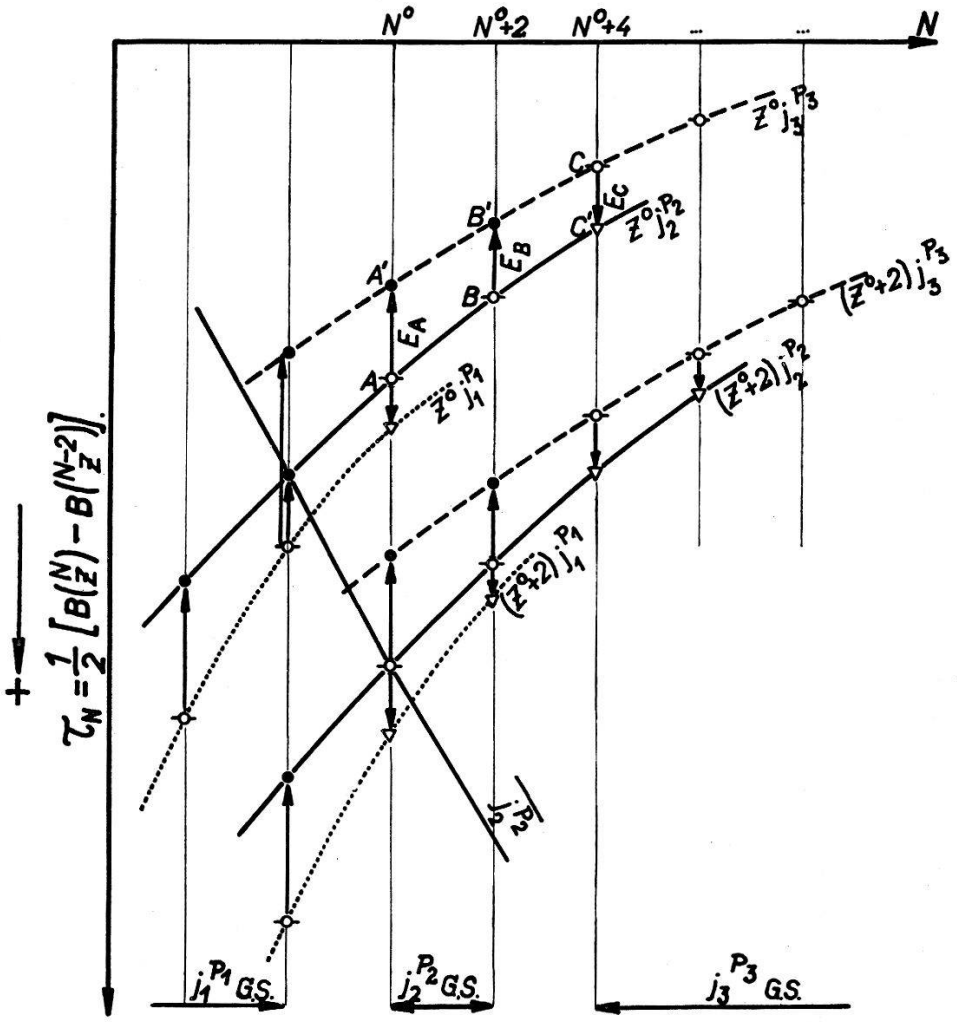

Fig. 2.

The method of construction of the diagram (schematic).

Various nuclei with N^0-2, N^0, N^0+2... neutrons and Z^0, Z^0+2 protons are considered. The assignments of their states are denoted by $j_1^{P_1}$, $j_2^{P_2}$, $j_3^{P_3}$. First, we construct the ground state points -o- (A, B, C etc.) with the help of the corresponding ionization energies τ_N (plotted on the vertical axis in the downward direction). Next, the excited states are inserted by means of the excitation energies. For the ordinary excited states • (A', B') we draw the excitation energies (E_A, E_B) in the upward direction from the corresponding ground state points. For the hole states ▽ (C') we choose the opposite direction. Eventually, all points (ground states and both kinds of excited states) which correspond to the same assignment jP and to the same proton number Z are connected by smooth curves. This system K_{ZjP} of curves is drawn for two values (Z^0, Z^0+2) for the proton number, and three different assignments. We have also drawn a short piece of the mean value curve $\overline{K}_{jP}$ corresponding to the assigment $j_2^{P_2}$. On the horizontal axis the different ground state regions (G. S.) have been indicated.

B. *Extension with the help of excited states.*

A large number of excited states with a known assignment can now be plotted in our diagram (fig. 2): The excitation energy is drawn along the vertical axis starting from the corresponding ground state point. The sign is negative for ordinary excited states (higher levels in the shell structure) and positive for so called hole-states. In most cases this important distinction can also be made with the help of a phenomenological criterium: Sign minus if in the surrounding region the ground states with the same assignment occur predominantly at the right hand side (larger N) and sign plus if the corresponding ground states are situated on the left. In fact, most of these new points lie on the extension of our curves K_{Zj^P}. This fact again corresponds to the special properties of ideal shell structure: A single particle level appears alternatively as an excited state, ground state and hole state if the neutron number increases (compare fig. 1). This behaviour, however, might be changed to a certain extent by the perturbating direct interactions which must yet be taken into account. It is, therefore, a remarkable experimental result that these general properties of continuity are still maintained, i.e. that a large percentage of all experimental ground states*) and low-lying excited states are embedded into this enlarged scheme. This proves our conjecture, mentioned in section 1, about the influence of the perturbations for a large part of the periodic table. This situation, however, is completely changed in the region of deformed nuclei and for higher excited states.

Some general features of our enlarged system (e.g. the average values for the gradients of our curves) also correspond to the well known properties of the surface representing the 'valley of binding energies' $B(N.\,Z)$. (Binding energy B plotted as a function of N and Z in a 3-dimensional space.) This function may also be expressed in analytical form[5]). The separation energies τ are then approximately determined from the expression $\partial B/\partial N$ (compare (1)). Our system reveals, however, that the energy surface B for odd nuclei is split into several layers B_{j^P} each corresponding to one of our sub-systems, characterized by a fixed assignment j^P. In addition, there are larger irregularities (ridges) along the lines determined by the magic numbers. Unfortunately it is very difficult to give a complete (3-dimensional) representation of these facts. We therefore construct our condensed '2-dimensional' scheme.

*) There are well known exceptions in the middle regions of the $9/2^+$ and $7/2^-$ shells the experimental assignment being $7/2^+$ instead of $9/2^+$ and $5/2^-$ instead of $7/2^-$.

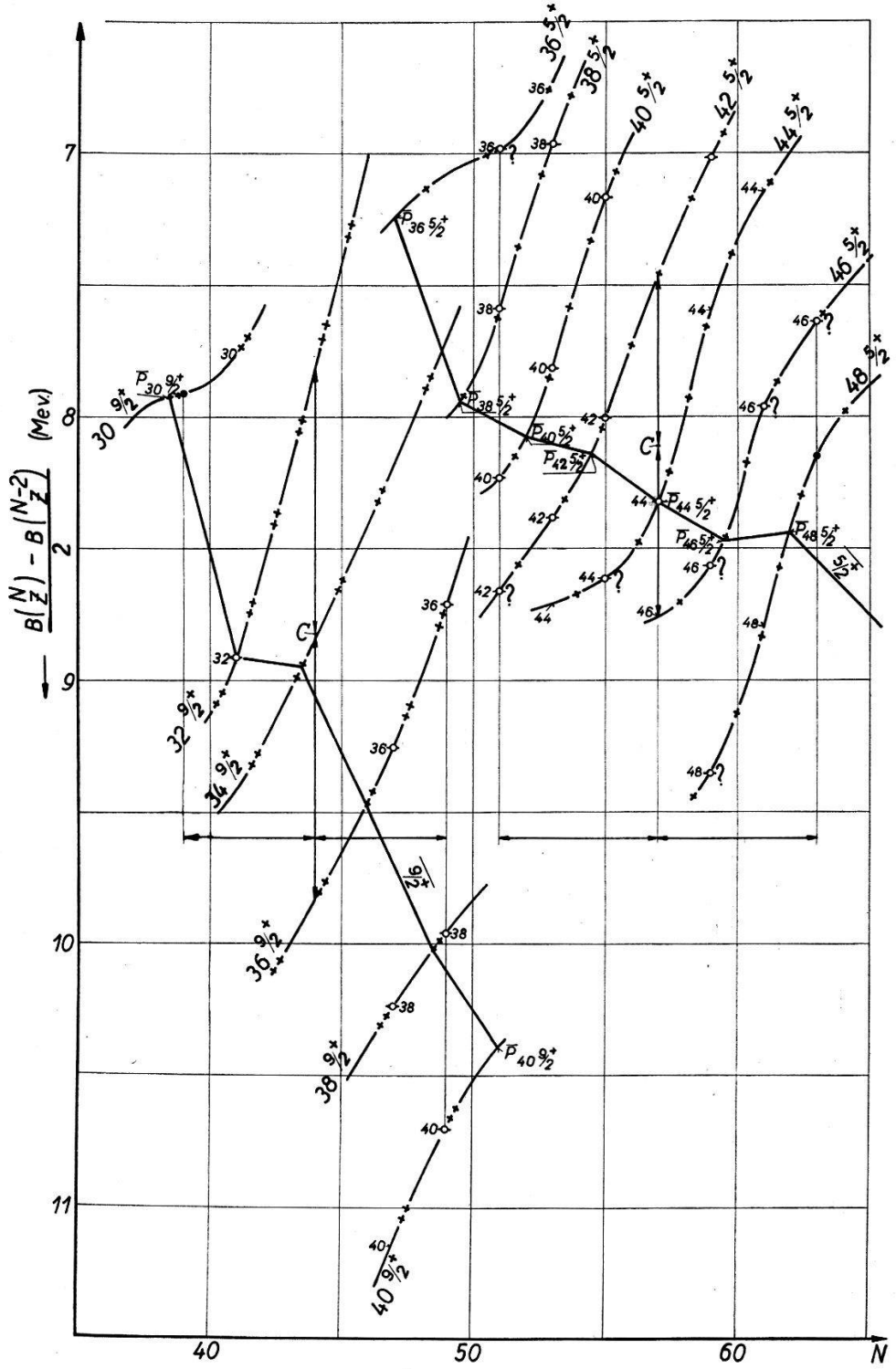

Fig. 3.

Part of the actual representation of levels for the region $N = 35$—65.

The broken curves represent our systems K_{Zj^P}. Only the two assignments $j^P = 5/2^+$ and $9/2^+$ are considered here. The points C are the centres of gravity of all measured points of the two systems. They were used for the construction of tangents in Fig. 4. The full lines are the mean value curves $\overline{K}_{j^P}$ for our two systems. The same symbols as in Fig. 1 are used for the nuclear states (o = ground state). States without measured assignment are indicated by the corresponding number Z. The curve for $Z = 34$ should be discarded.

C. *The mean value curves.*

In the (N, Z)-plane we now consider the distribution of all stable elements. We then draw an analytical curve (expressed by the function $\overline{N}(Z)$), representing the 'middle line' of this distribution (in the same time the projection of the bottom of the energy valley $B(NZ)$). With the help of this line we construct a 'central point' $\overline{P}_{Zj^P}$ on each curve K_{Zj^P} of our system: The abcisse $\overline{N}$ is determined by the mean neutron number $\overline{N}(Z)$ corresponding to the proton

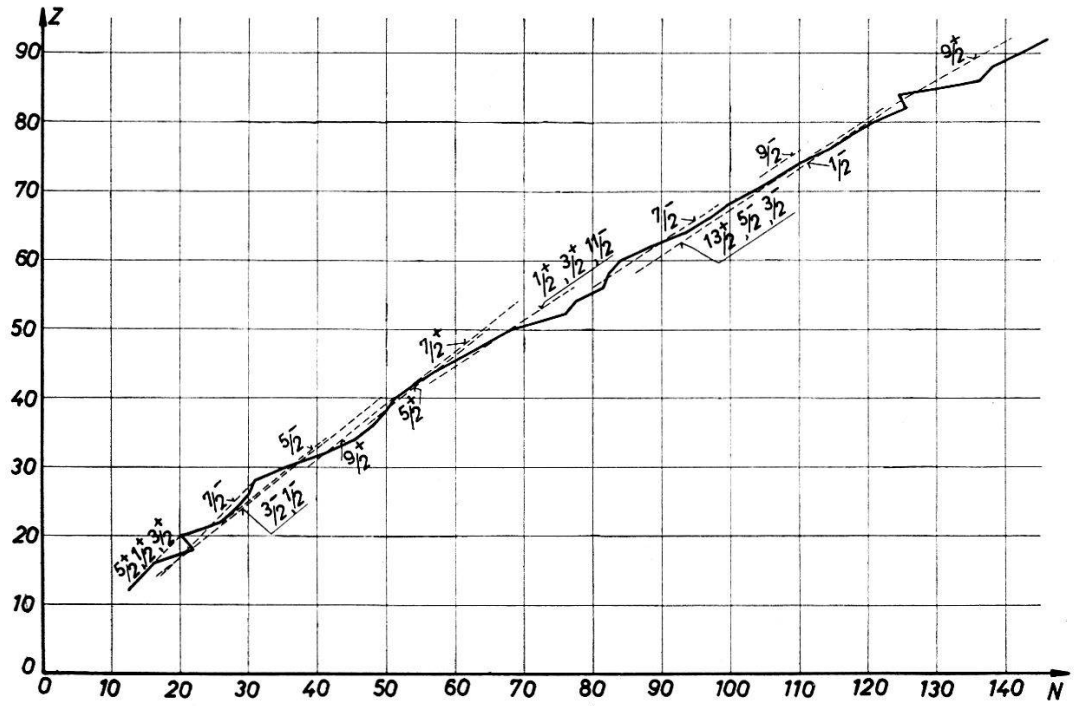

Fig. 4.

The Distribution of the stable elements.

The full drawn curve is plotted along the centres of gravity of all isotopes on an horizontal line (fixed, even Z, weight according to abundance). Dotted lines: Tangents to an averaged middle line $\overline{N}(Z)$ used for the determination of the mean value curves.

number Z of our curve; the coordinates of $\overline{P}_{Zj^P}$ in our (τ, N)-plane are, therefore, $\tau_{j^P}(\overline{N}(Z), Z)$ and $\overline{N}(Z)$ respectively, (compare fig. 3).

It may now be seen that all points $\overline{P}_{Zj^P}$ which belong (in a certain region) to the same assignment j^P (i.e. to the same sub-system) in fact lie on smooth curves $\overline{K}_{j^P}$. In this way we obtain our new system of mean value curves $\overline{K}_{j^P}$. Each $\overline{K}$ corresponds to one of our sub-systems (characterized by the assignment j^P) which in turn represents an energy surface $\tau_{j^P}(N, Z)$. It is, therefore, easily seen that

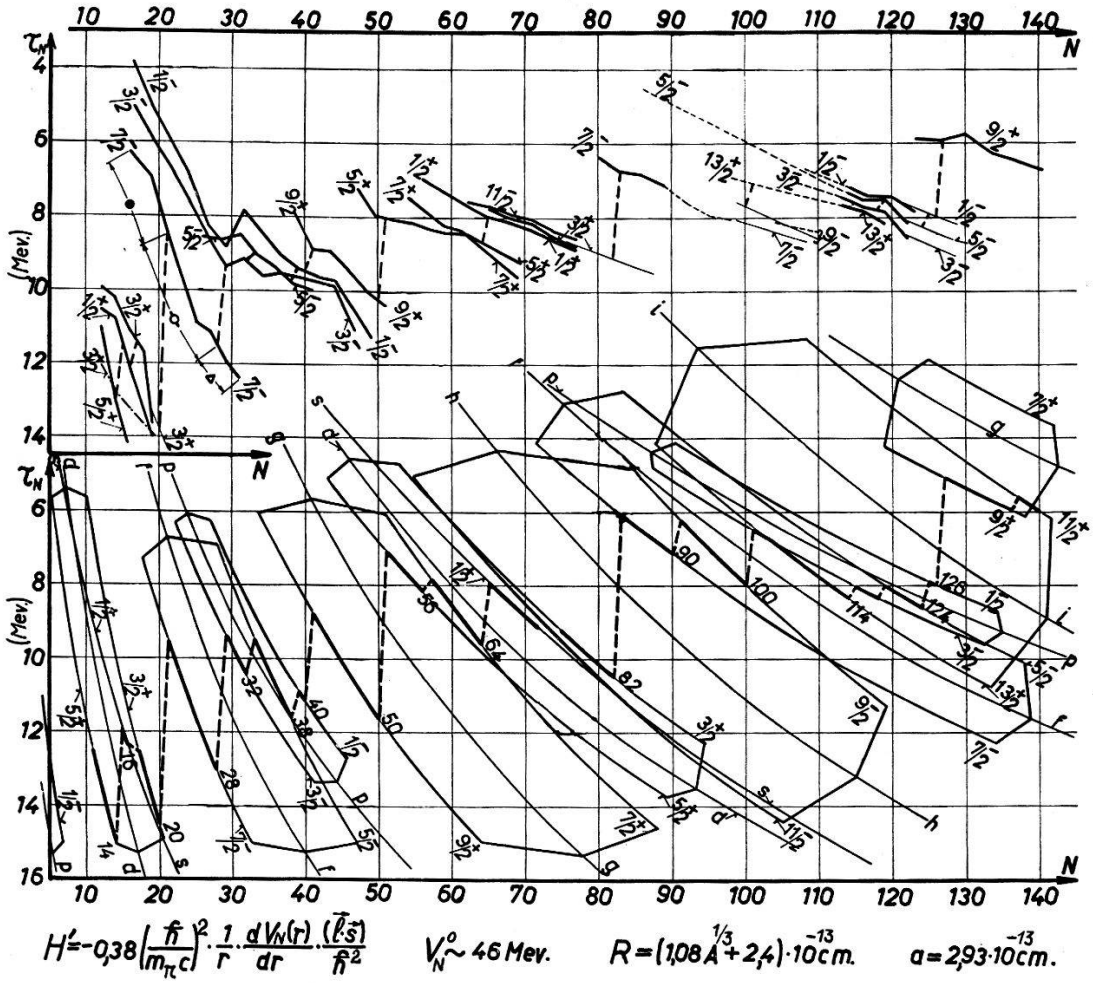

Fig. 5.

The comparison between the experimental data and the single particle levels of the shell model (energy levels as functions of N).

In the top part the experimental data are represented with the help of our mean value curves $\overline{K}_{jP}$ (compare figs. 2 and 3). The thin dotted extensions of these curves are interpolated (lack of experimental evidence). On the $7/2^-$ curve we have indicated the different domains corresponding to hole states (∇), ground state (-o-) and excited states ($\bullet$). The heavy dotted lines always connect the end of the ground state region on one curve with the beginning of this region on the next mean value curve. The length of each curve is determined by β-instability. The curves for the assignments $11/2^-$, $3/2^+$ and $1/2^+$ stop suddenly for $N = 76$. This results from the fact that the corresponding Z lies in the neighbourhood of the magic number 50. There is, therefore, a sudden rise of the highest proton level which causes β^+-instability of the odd N isotopes. We have inserted a continuous prolongation (thin line) in order to show more clearly the energetic step for $N = 82$. There is a similar situation near $N = 126$.

In the lower part the theoretical one particle levels are drawn. The parameters of the corresponding nuclear potentials and the spin orbit interaction are indicated. The thick lines represent the highest occupied levels (for ground states), the thinner extensions correspond to excited levels. At the lower end of the thin lines the spin orbit splitting is indicated.

this explicit construction of the $\overline{K}$-system is equivalent to the more geometric definition given in section 1 where the same middle line $\overline{N}(Z)$ has been used.

For practical reasons $\overline{N}(Z)$ was approximated by a series of straight lines (compare fig. 4), each line corresponding to one of our sub-systems. They were determined by the following conditions: (a) The $\overline{K}$-curves should contain some points $\overline{P}$ which are directly measured. (b) The directions are essentially tangential to a smooth middle line $\overline{N}(Z)$. (c) They are situated in the center region of the nuclear distribution in the (N, Z)-plane (the centers of gravity C of the distributions corresponding to one assignment were used; see fig. 3).

Our new $\overline{K}$-curves are shown in the upper part of fig. 5 for the whole periodic system. On most of them we can define a middle region which corresponds to the ground states of the generating nuclei. These regions are marked by nearly vertical dotted lines which connect the end of the middle region on one curve with the beginning of the ground state region on the following curve. The lengths of these dotted lines, therefore, represent the average differences of ionization energies of neighbouring nuclei corresponding to different assignments. These energy steps are much larger at the position of the magic numbers. The $\overline{K}$-system constitutes the main result of our geometry of nuclear levels. It provides an intuitive survey of nuclear properties and a basis for our comparison.

§ 3. Comparison with the shell model.

A. *The shell structure.* All nucleons are assumed to move independently within a spherically symmetric nuclear potential $V(r)$; a large spin orbit term H' must be taken into account. Therefore, we have to determine the eigenvalues E_n of the operator

$$-\frac{\hbar^2}{2m}\Delta + V + H' \tag{2}$$

for the complete sequence of nuclear potentials V which occur in the periodic system. The form of V is shown in fig. 6; it is determined by 3 parameters: Radius R, depth V_N^0 and the inclination of the walls a (diffuseness of the surface). The first task is the determination of the eigenvalues E_n as functions of these parameters. These rather lengthy calculations (including a rigorous treatment of the spin orbit

term) were accomplished with the help of a graphical method outlined in I*).

The definition of the potential, however, is somewhat different from the one used in the previous paper (I): $V(r)$ now represents, as usual, the whole one particle potential generated by the remaining nucleons in the lowest bound state**).

In view of this definition of V the ionization energy can be determined directly (distance between the last occupied level from the the zero line of V (compare fig. 6)). We assume different potentials for protons and neutrons respectively. The parameters of our neutron potentials were determined by means of the following assumptions:

(a) The radius law $R(A)$ was taken from the new HOFSTADTER[6]) results; a constant was added in order to allow for the finite range of nuclear forces (see fig. 6).

$$R = (1.08\, A^{1/3} + 2.4) \cdot 10^{-13} \text{ cm}. \tag{3}$$

(b) The surface diffuseness was assumed constant according to the Hofstadter result for the charge distribution.

$$a = 2.9 \cdot 10^{-13} \text{ cm}.$$

(c) For the depth $V_N^0(A)$ we chose a smooth function which was determined indirectly from our experimental values of the ionization energies. For this purpose the experimental values (according to fig. 5) were represented by a smooth overall mean value curve which had to coincide with the corresponding curve from the theoretical diagram. It is a striking fact that we found a nearly constant value for V_N^0 (i.e. independent of A for $A > 40$, say):

$$V_N^0 \approx 46 \text{ MeV}.$$

This result is in agreement with the constant values of the nuclear densities. (This fact constitutes an indirect check for the validity of the new radius law (3) and the consistency of this model; according to our method the values obtained for $V_N^0(A)$ depend in a rather sensitive manner on the numerial factor in the $A^{1/3}$ term). On the other hand our $V(r)$ agrees fairly well with the result of the WEISSKOPF-FESHBACH[7]) analysis of neutron scattering experiments.

*) This new evaluation has been performed by Mr. A. SCHRÖDER.

**) In paper I the potential was normed in a different way: The depth of the well represented the potential energy per nucleon corresponding to simultaneous discarding of all particles. In this case the sum of the energy-eigenvalues of all nucleons represents the total binding energy of the nucleus. This is no longer the case if we introduce the present definition.

(d) We choose the following expression for the spin orbit term H':

$$H' = -0.38\left(\frac{\hbar^2}{m_\pi c}\right)^2 \frac{1}{r}\frac{dV}{dr}\frac{1}{\hbar^2}(\vec{l}\vec{s}) \tag{4}$$

(The Compton wave length of the π-meson was introduced for dimensional reasons. The splitting is proportional to l and the gradient of the nuclear potential.) This expression was determined by trial from a comparison with the experimental results (see below). The constant dimensionless factor (0.38) which describes the absolute magnitude of this interaction, constitutes a lower limit: Constant values up to 0.45 might still be compatible with our analysis*).

In the lower part of fig. 5 we have plotted the results of these calculations (theoretical two-dimensional level scheme for ideal shell structure). All eigenvalues are drawn as functions of N and the corresponding quantum numbers j^P are indicated on each curve. (A is

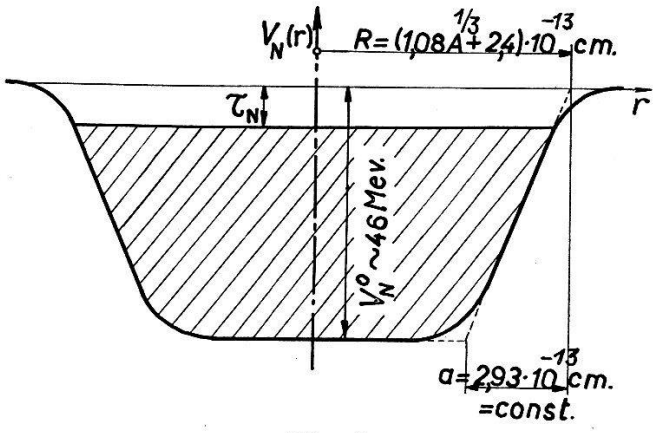

Fig. 6.
The shape of the nuclear potential.
Definition of the parameters R, V_N^0 and the slope a. Shaded area: occupied levels. τ_N = ionization energy (separation energy).

expressed as a continuous function of N by means of our middle line $\bar{N}(Z)$.) The heavy lines indicate the position of the highest occupied level in the ground state (Fermi energy). The dotted lines again indicate that a level has been occupied completely and that a higher one is needed. The extensions of the heavy lines represent excited single particle states. Thus our system shows the behaviour of the ideal one-particle levels for all nuclei situated within the 'middle line' of the distribution of stable elements; it will now be compared to the corresponding experimental system constructed in the previous section.

*) The result of KÖHLER and ERIKSSON[10]) is 0.33 in our units. These authors, however, used a flatter shape for the nuclear potential. For this reason a somewhat smaller value for the coupling constant must be expected.

B. *The comparison.* The similarity of the two systems of curves is really striking: There is in fact a perfect one to one correspondence which could hardly be expected to hold to this extent (the theorectical curves representing merely single particle states):

(a) To every theoretical curve there corresponds an experimental one with the same assignment and nearly the same energetic position. We have, in general, the same sequence (from left to right) of excited states, ground states and hole states in both systems of curves.

(b) The inclination of the experimental curves is smaller in all cases: This constitutes the effect of a certain amount of admixtures to our single particle states. On the other hand, the continuous decrease of the inclinations for increasing A corresponds perfectly to the behaviour of the ideal single particle curves.

(c) The typical energetic steps at the position of the magic numbers (20, 28, 50, 82, 126) are somewhat smaller than the theoretical ones (admixtures), but their ratios are nearly equal throughout the periodic table. This fact was important for the determination of the law for the spin orbit coupling. More details about this point will be given in a subsequent paper.

Eventually, we consider the experimental level schemes of the three ideal cases (double magic plus one, i.e. small admixtures):

$$Ca^{41},\ Ca^{49},\ Pb^{207}.$$

The following table gives the calculated and experimental[12)13)] excitation energies. Again, the theoretical values are based on our graphical integration method (results from fig. 5).

Table I.

	Ca^{41}		Ca^{49}		Pb^{207}	
	exper.	theor.	exper.	theor.	exper.	theor.
Ground state	$7/2^-$	$7/2^-$	$3/2^-$	$3/2^-$	$1/2^-$	$1/2^-$
exited states	$3/2^-$, 1.95	$3/2^-$, 3.5	$(1/2^-)$, 2.02	$1/2^-$, 2.2	$5/2^-$, 0.57	$5/2^-$, 0.8
(exitation					$3/2^-$, 0.90	$3/2^-$, 1.1
energies					$13/2^+$, 1.63	$13/2^+$, 1.9
in Mevs)	$(1/2^-)$, 2.49	$1/2^-$, 5.7			$7/2^-$, 2.35	$7/2^-$, 3.5

The agreement is particularly good for large A and small excitation energies. For higher excitation pure single particle states can no longer be expected. It is clear, therefore, that the discrepancies always become larger for higher energies. (Ca^{41} is a typical example.)

In addition, it should be borne in mind that our graphical determination becomes rather inaccurate for the levels lying near the ionization edge.

In the region $N = 90$—115 ($Z = 60$—75) there are characteristic differences between the theoretical results from the spherical shells and the experimental values. This is just the region where the highest density of the single particle levels occurs. For this reason spherical structure may become rather unstable. It is a striking fact that nuclear deformation appears in this region. Unfortunately there are too few experimental values for binding energies in this domain. Therefore, large parts of the curves had to be interpolated (dotted). In the region $N = 70$—80 we find for the first time a larger level density: yet, the correspondance of our two schemes is quite good but the quadrupole moments are already much larger than the corresponding single particle values.

It still remains an outstanding result that, in a large region of the periodic system, nearly all low-lying nuclear states (only the $7/2^+$ levels in the $9/2^+$ shell and $5/2^-$ levels in the $7/2^-$ shell are exceptions) can be approximately described by one particle states, even in the case of half filled shells where very different assignments might be expected. Eventually, our theoretical single particle level scheme might represent a common basis for the theoretical calculations needed in order to determine the effect of the direct interaction between nucleons.

§ 4. Light nuclei and spin orbit coupling.

It has been seen from our comparison that the structures of most of the heavier nuclei (A above 30) are rather similar. This striking fact is already suggested by the existence of continuous curves connecting corresponding levels. The situation, however, is very different for light nuclei: A glance at their level schemes[8]) will immediately show that smooth curves, in the former sense, no longer exist. Therefore, it will be interesting to decide whether the same expression (4) for our spin orbit interaction still holds in this region. Although the accurate structure of light nuclei is unknown, there are three pairs of mirror nuclei:

$$He^5\ Li^5;\quad C^{13}\ N^{13};\quad O^{17}\ F^{17}$$

for which one may assume an alcalide structure: There is a stable core (He^4, C^{12}, O^{16}) surrounded by an extra nucleon. The ionization energy for the extra particle as well as the spacing of the lowest

levels are small (although not extremely small) in comparison to the excitation energy of the corresponding core. From these merely experimental facts the alcalide structure is quite obvious: The extra nucleon is moving in the potential field generated by the core. This field is spherically symmetric, the cores having spin zero in all cases. Therefore, our spin orbit interaction term may be applied in exactly the same form as in section 3.

A more mathematical treatment of these nuclear alcalides was given by one of us[9]). The main point was a development of the stationary state ψ_m of the complete system with the help of the stationary states φ_n of the core:

$$\psi_m(x, x_1 \cdots x_N) = \sum_n C_m^n(x)\, \varphi_n(x_1 \cdots x_N) \tag{5}$$

($x_1 \ldots x_N$ represent the position and spin variables of the nucleons of the core; x is the variable of the extra particle; it plays formally the role of a parameter in this development.) The coefficients $C(x)$ can now be interpreted as wave functions of the extra particle. Our scope is to obtain an equation for these functions alone. For this reason we split the hamiltonian H of the system into two parts in order to introduce the hamiltonian H^0 of the core for which the eigenfunctions φ_n and the eigenvalues E_N^0 are assumed to be known.

$$H = H^0 + H^1 . \tag{6}$$

From a generalized perturbation theory with respect to the operator H^1 we obtain the following result: In the lowest approximation the expression (5) for ψ contains only one term:

$$C_m^{n_0}\, \varphi_{n_0}(x_1 \cdots x_N) \tag{7}$$

That means the core remains in the state n_0; it is surrounded by an extra particle described by the wave function $C_m^{n_0}(x)$ determined by a single particle equation containing the central field generated by the core. In the higher approximations, however, further terms of the development (5) will occur. These terms represent admixtures (including the core excitation) which play a rather important role in nuclear structure in contrast to the case of atomic alcalides. In order to satisfy to the exclusion principle in all approximations, our expression (5) has still to be antisymmetrized. For this reason the hamiltonian which describes the extra particle contains, apart from an ordinary central potential with our spin orbit coupling, also an exchange integral operator which is due to this antisymmetrization. From some considerations concerning the structure of the core (the

wave function of the core must be developed with the help of the orbitals of our central potential), it appears that these special exchange operators are of importance only for a few low-lying states $C_m^{n_0}$ of the extra particle (those whose wave functions have large coefficients in the development of the core). The remaining states, therefore, are approximately described by the same hamiltonian which we have used already in section 3. In fig. 7 we have indicated the experimental values for the levels in question (the corresponding levels from mirror nuclei nearly coincide, fig. 8). Several levels (dotted lines, fig. 7) are expected to be strongly shifted by the exchange integral operator; they will be discussed in a later publication. All remaining levels are indicated by heavy lines. These values will be compared to the results from our calculations.

For this purpose, we made some natural assumptions about the nuclear potential generated by the cores (compare fig. 9 left bottom corner). We then applied our former spin orbit term (4) with the same numerical value for the magnitude of the coupling. The parameters of our potentials are partly determined by the known separation energies and by some approximate values for the radii. Again, we used our graphical integration method. The result is shown in fig. 9 (thin curves; their intersections with the vertical lines have to be compared with the horizontal bars). There is a good agreement in nearly all cases. (The $7/2^-$ state in O^{17} shows a rather large displacement due to higher admixtures.)

Combining these facts with the results from section 3, we may conclude that the spin orbit interaction is a characteristic, intrinsic property of the nuclear field. In order to make a preliminary estimate, we replace our nuclear potential by a classical meson field. If we choose a scalar field V we have the following relativistic equation for the nucleon moving in V:

$$c\left(\frac{\hbar}{i}\frac{\partial}{\partial x_\mu}\gamma_\mu\right)\psi + mc^2\,\psi + V\psi = 0\,. \tag{8}$$

In the Pauli approximation a spin orbit interaction does, in fact, appear as a relativistic correction, but, as is well known, this term is far too small. The situation, however, is quite different if we introduce a pseudoscalar meson field V':

$$c\left(\frac{\hbar}{i}\frac{\partial}{\partial x_\mu}\gamma_\mu\right)\psi + mc^2\,\psi + V'\gamma_5\,\psi = 0\,. \tag{9}$$

Now, the unrelativistic approximation contains, already in the lowest order, a spin dependent term:

$$(\vec{\sigma}\ \overrightarrow{\text{grad}}\ V')\,\psi. \tag{10}$$

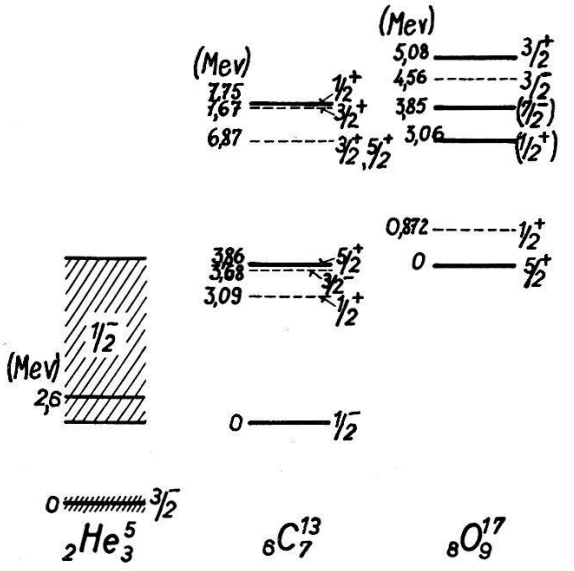

Fig. 7.

Levels of nuclear alcalides (according LAURITSEN *et al.*[8])).

The dotted lines indicate levels which are supposed to be strongly shifted by the exchange integral operator. The full lines represent the levels used for our comparison with the calculations.

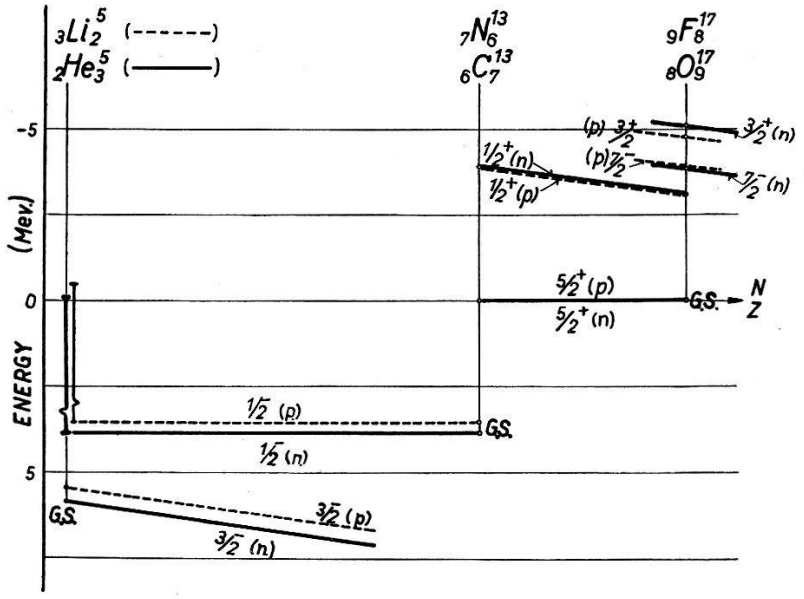

Fig. 8.

Levels of mirror nuclei.

Full lines: levels of the extra neutron; dotted lines: extra proton. The $5/2^+$ levels coincide by construction. The proton levels are slightly compressed with respect to the corresponding neutron levels. This constitutes an effect of the Coulomb energy.

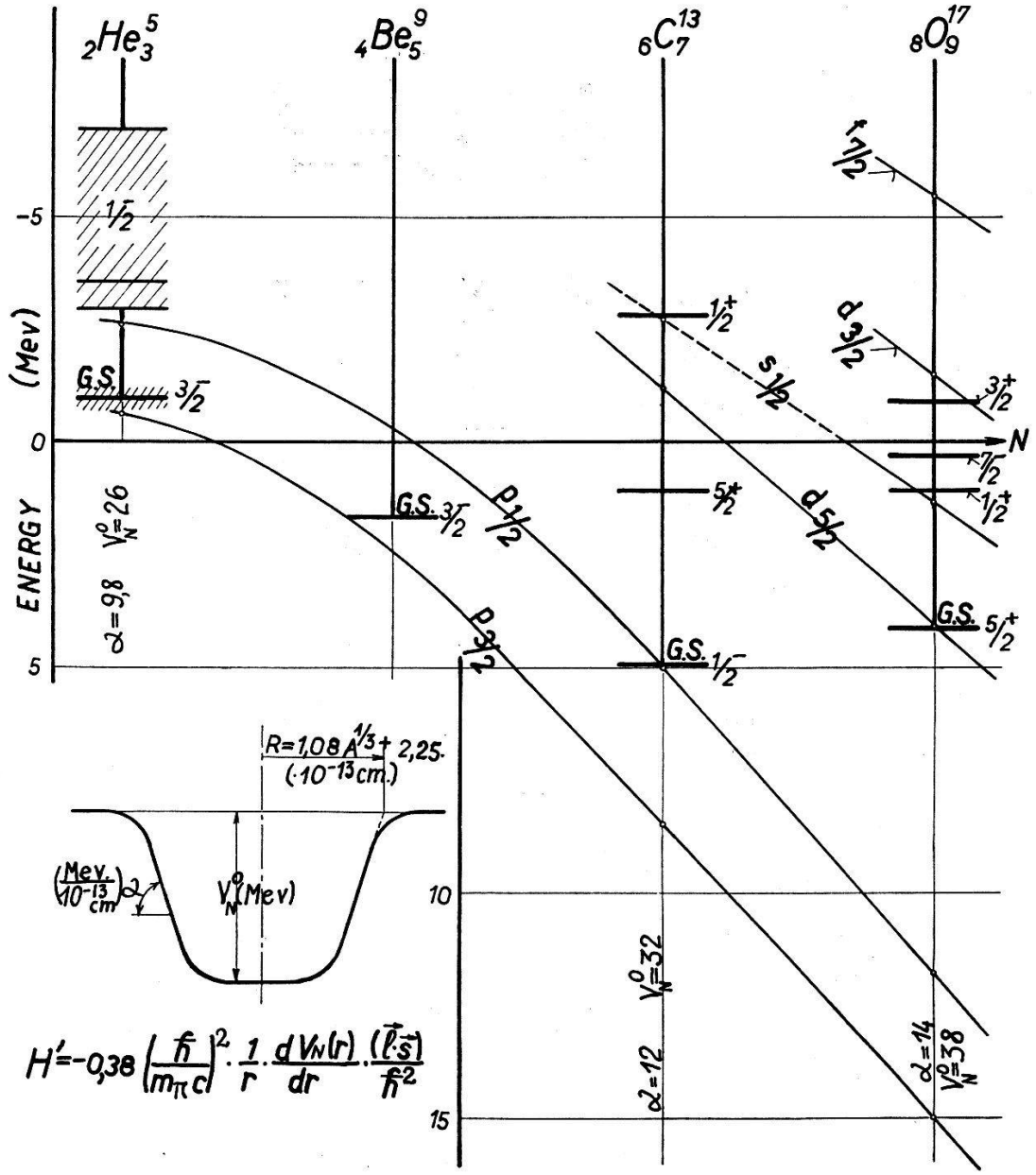

Fig. 9.
Theoretical and experimental levels for light nuclei.

Horizontal bars: experimental (according to Fig. 7). G. S. = ground states (position determined by the ionization energy).

Continuous curves: results from the calculations. The intersection with the vertical lines should be compared with the (experimental) horizontal bars.

Left bottom corner: Potentials generated by the cores used for our calculations (including the spin orbit interaction H').

At first sight, this expression does not have the form of an ordinary spin orbit interaction. It seems, however, very likely that the sequence of one particle levels obtained from (10) is quite similar to the spectra calculated in section 3. The pseudoscalar theory of the nuclear field has some interesting features concerning the definition of

the parity of states: The whole system composed of nucleons and the meson field must be considered for this purpose. There will be a mixing between even and odd single particle states which might throw some light on the properties of nuclear magnetic moments. Thus, this paper constitutes the basis for further work.

Acknowledgements: As far as one of us (T) is concerned, the work was carried out with the help of a grant by the "Schweizerische Nationalfond". For this we should like to express our thanks to the "Forschungsrat". To Mr. A. SCHRÖDER we are indebted for a new evaluation of the energy levels.

References.

[1]) KLINKENBERG, P. F. A., Rev. Mod. Phys. **24,** 63 (1952).
[2]) BLEULER, K., and TERREAUX, Ch., Helv. Phys. Acta **28,** 245 (1955), here quoted as I.
[3]) WAPSTRA, A. H., Physica **21,** 367, 385 (1955).
[4]) HUIZENGA, J. R., Physica **21,** 410 (1955).
[5]) BETHE and BACHER, Rev. Mod. Phys. **8,** 82 (1936).
[6]) HAHN, B., RAVENHALL, D. G., and HOFSTADTER, R., Phys. Rev. **101,** 1131 (1956).
[7]) FESHBACH, H., PORTER, C. E., and WEISSKOPF V. F., Phys. Rev. **96,** 448 (1954).
[8]) AJZENBERG,F., and LAURITSEN, T., Rev. Mod. Phys. **27,** 77 (1955).
[9]) BLEULER, K., Proceedings of the 1954 Glasgow Conference on Nuclear and Meson Physics, p. 132.
[10]) ERIKSSON, T., Nuov. Cim. **2,** 907 (1955); KÖHLER, S., Nuov. Cim. **2,** 911 (1955).
[11]) BOHR, A., Dan. Mat.-fys. Medd. **26,** No. 14 (1952); BOHR, A., and MOTTELSON, B. R. Dan. Mat.-fys. Medd. **27,** No. 16 (1953); BOHR, A., Rotational states of nuclei København 1954; GOTTFRIED, K., P. R. **103,** 107 (1956); MOSZKOWSKI, S. A., P. R. **103,** 1328 (1956); F. VILLARS, Phys. Rev. (to be publ.)
[12]) ALBURGER, D. E., and SUNYAR, A. W., P. R. **99,** 695 (1955).
[13]) NUSSBAUM, R. H., Thesis Amsterdam University (1954). Nuclear Levels in the neighbourhood of the 1 f $_{7/2}$ state; BRAAMS, C. M., Thesis Utrecht University (1956). Energy levels of calcium isotopes; BRAAMS, C. M., P. R. **103,** 1310 (1956).
[14]) KATHERINE WAY a. o., Nuclear Data.

*